INVERSE DYNAMICS OF A 3 DEGREE OF FREEDOM SPATIAL FLEXIBLE MANIPULATOR

E. Bayo and M. Serna

Department of Mechanical Engineering
University of California
Santa Barbara, CA 93106

Abstract

A technique is presented for solving the inverse dynamics and kinematics of 3 degree of freedom spatial flexible manipulator. The proposed method finds the joint torques necessary to produce a specified end effector motion. Since the inverse dynamic problem in elastic manipulators is closely coupled to the inverse kinematic problem, the solution of the first also renders the displacements and rotations at any point of the manipulator, including the joints. Furthermore the formulation is complete in the sense that it includes all the nonlinear terms due to the large rotation of the links. The Timoshenko beam theory is used to model the elastic characteristics, and the resulting equations of motion are discretized using the finite element method. An iterative solution scheme is proposed that relies on local linearization of the problem. The solution of each linearization is carried out in the frequency domain.

The performance and capabilities of this technique are tested through simulation analysis. Results show the potential use of this method for the smooth motion control of space telerobots.

1. Introduction

The assumption that robot arms are rigid is not valid when considering light manipulators handling heavy payloads with accuracy. In modelling and controlling these manipulators the flexibility of their members must be considered. In particular, residual vibrations must be avoided when positioning the end-point of a robotic arm. Different techniques, too numerous in fact to be mentioned here, have been proposed to achieve this goal. They differ in the mathematical model used to describe the dynamics of the system, and by the sensors and control laws used to achieve the overall motion of the arm while controlling the tip vibrations [1-5].These results show either an initial motion of the tip in the opposite direction of the overall motion (undershoot) or an overshoot of the set-point and residual vibrations at the end of the trajectory. The initial undershoot is characteristic of the step response of a non-minimum phase system, such as a flexible link [1-5]. By relying entirely on feedback schemes, the mentioned techniques implicitly considered causal controls.

The authors introduced a direct approach for the solution of the inverse dynamics of a single-link [6,7], and multi-link [8] flexible manipulators. The proposed method finds the joint torques necessary to produce a desired end effector motion. The new technique for inverse dynamics has been validated by feed-forwarding the computed torques in numerical simulations [6-8], and in experiments [7,8] for both single and multi-link planar flexible robots, yielding excellent results. For a generic acceleration profile the solution of the inverse dynamics yields a torque that must be applied before the end-effector starts actually moving. The inverse dynamics provides a unique non-causal control law [9] which is capable of tracking a specified trajectory with no deflections from it. In particular, it is possible to track any Fourier transformable acceleration profile with zero initial undershoot or overshoot, and this therefore contradicts the belief that a non-minimum phase system can not be inverted for any given trajectory [10]. This only applies if causal solutions are sought, as is the case in Ref. [10].

In this paper that formulation is extended to compute the joint torques (and joint angles) that position the end-effector of a 3 degree of freedom spatial flexible manipulator along prescribed trajectories. The new formulation includes all the nonlinear Coriolis and centrifugal effects. Timoshenko beam theory is used to model the elastic behavior of the system and the resulting

equations of motion are discretized using the finite element method. An iterative solution scheme is proposed for finding the desired joint torques, where the solution of each linearization is carried out in the frequency domain. A simulation is performed that demonstrates the capabilities of the present formulation in handling the problems of vibration control and trajectory tracking of spatial manipulators. The technique is therefore of direct use for open-loop control and it also provides the basis for closed-loop control algorithms.

2. Kinematics

Let us consider the spatial manipulator depicted in Fig. 1 that has three degrees of freedom and three revolute joints. The objective is to move the end effector along a given trajectory without overshoot and residual elastic oscillations of the tip. These oscillations are due mainly to the transverse elastic displacements of the links. We consider the case in which a general three dimensional motion is decomposed into three parts as shown in Fig. 2. The first and third parts are planar motions and involve the rotations about the Z_2 and Z_3 axis. The second part of the motion is composed of a rotation about the Z_1 axis.

Kinematics of the first and third motion

The first and third parts of the motion are planar. Consider the individual flexible link depicted in Fig. 3 of total length Lthat forms part of the spatial robot. A point P at a distance x from the center of the hub has undergone elastic deflections of value u_x and u_y, and rotation θ. These are defined with respect to a nominal position characterized by the moving frame $(\bar{e}_1, \bar{e}_2)$ that rotates at a specified nominal angular velocity and acceleration ω_n and α_n, respectively. This definition of the motions with respect to the nominal frame permits the linearization of the problem from the outset.

As a consequence of the elastic deflections and rotating nominal motion, the point P is subjected to a total linear acceleration a_p and angular acceleration α_p. The acceleration of the point P can be set in terms of the nominal translational and angular accelerations at the hub, a_n and α_n, angular velocity ω_n at the hub, and the relative velocity v_{rel} and acceleration a_{rel} of the point P. The latter are due to the elastic deflections with respect to the moving frame. The kinematics of the motion can be established as follows:

$$a_p = \omega_n \times (\omega_n \times r) + \alpha_n \times r + 2\omega_n \times v_{rel} + a_n + a_{rel} \qquad (1)$$

$$\alpha_p = \alpha_n + \ddot{\theta}$$

where $r = (x + u_x)\,\bar{e}_1(t) + u_y\,\bar{e}_2(t)$

The components of the relative velocity are $\dot{u}_x$ and $\dot{u}_y$, and those of the relative acceleration are $\ddot{u}_x$ and $\ddot{u}_y$. Performing the vectorial operations involved in Eq. (1) the following components of the accelerations are obtained:

$$\begin{aligned} a_x &= -\omega_n^2 u_x - \alpha_n u_y - 2\omega_n \dot{u}_y + \ddot{u}_x - \omega_n^2 x + a_{nx} \\ a_y &= \alpha_n u_x - \omega_n^2 u_y + 2\omega_n \dot{u}_x + \ddot{u}_y + \alpha_n x + a_{ny} \\ \alpha_p &= \alpha_n + \ddot{\theta} \end{aligned} \qquad (2)$$

Kinematics of the second motion

Fig. 4 shows the deformation of the manipulator in this second part of the motion which consists in a rotation about the global y axis. The position vector for the point P now becomes.

$$\boldsymbol{r} = (x + u_x)\,\bar{e}_1 + (y + u_y)\,\bar{e}_2 + u_z\,\bar{e}_3 \tag{3}$$

Note that the moving frame is now $(\bar{e}_1, \bar{e}_3)$ which rotates about the y axis, hence the vectors ω_n and α_n contain only one non-zero component. Again performing the vectorial operations involved in Eq. (1) the following six components of the accelerations are obtained.

$$\begin{aligned} a_x &= -\omega_n^2 x - \omega_n^2 u_x + \alpha_n u_x + 2\,\omega_n \dot{u}_z + \ddot{u}_x , & \alpha_x &= \ddot{\theta}_x \\ a_y &= \ddot{u}_y , & \alpha_y &= \alpha_n + \ddot{\theta}_y \\ a_z &= -\omega_n^2 u_z - \alpha_n x - \alpha_n u_x - 2\,\omega_n \dot{u}_x + \ddot{u}_z , & \alpha_z &= \ddot{\theta}_z \end{aligned} \tag{4}$$

Note that this part of the motion has a full three dimensional behavior, and that in this case there is coupling between the x and z components of the motion through the elastic deformations.

3. Equations of Motion

Once the displacement field has been defined, the principle of virtual displacements can be used to directly set up the dynamic equations of motion. We rely on the Timoshenko beam theory, which includes the effects of shear deformation and rotatory inertia. For the general three dimensional case the equations become:

$$\int_0^L \left(\bar{m}\,[a_x, a_y, a_z] \begin{bmatrix} \delta u_x \\ \delta u_y \\ \delta u_z \end{bmatrix} + \bar{m}\,[\eta_x \alpha_x, \eta_y \alpha_y, \eta_z \alpha_z] \begin{bmatrix} \delta\theta_x \\ \delta\theta_y \\ \delta\theta_z \end{bmatrix} \right) dx + I_h(\alpha_n + \ddot{\theta}_h)\delta\theta_h + M_t a_t \delta u_t + \tag{5}$$

$$\int_0^L \left(E\left[I_y\,\theta_y', I_z\,\theta_z'\right] \begin{pmatrix} \delta\theta_y' \\ \delta\theta_z' \end{pmatrix} + GA\left[k_z\,(\theta_z - u_y'), k_y\,(\theta_y - u_z')\right] \begin{pmatrix} \delta(\theta_z - u_y') \\ \delta(\theta_y - u_z') \end{pmatrix} + EA u_x' \delta u_x' + GJ\theta_x' \delta\theta_x' \right) dx =$$

$$\boldsymbol{T}\,(\delta\theta_h - \delta\theta_t)$$

where η_x, η_y and η_z are the radii of gyration of the section, $\bar{m}$ the mass per unit length, I the moment of inertia, A the area, E the Young modulus, G the shear modulus and shear coefficient k. A tip masses are represented by M_t, and the hub inertias by I_h. δu_x, δu_y, δu_z, $\delta\theta_x$, $\delta\theta_y$ and $\delta\theta_z$ represent a set of virtual elastic displacements. $\boldsymbol{T}=(T_0, T_1, T_2)$ are the unknown torques to be applied at the different joints so that the prescribed end-effector motion is obtained. The equations of motion for the planar case (motions 1 and 3) can be obtained as a particular case of Eq. (5), and they are described in detail in [8]. Note that the accelerations at the joints will have two components α_n and $\ddot{\theta}$. The first are the nominal accelerations and the second are the acceleration due to the elastic deflections.

The displacement field of Eq (5) can be discretized using the finite element method. A complete set of interpolation functions are defined within each element:

$$u_j(x,t) = \sum_{i=1}^{n} H_i(x)\,u_j^i(t) \quad \text{and} \quad \theta_j(x,t) = \sum_{i=1}^{n} H_i(x)\,\theta_j^i(t) \tag{6}$$

where H_i are interpolation functions whose order depends on the number of nodes, n, in the elements; u^i_j and θ^i_j indicate the components j of the nodal deflections. Substituting Eq (4) and (6) in the virtual work expression, Eq (5), and following standard procedures for the formation and assemblage of element matrices [11], the equations of motion of the manipulator may be expressed by a set of time varying differential equations:

$$\mathbf{M}\,\ddot{\mathbf{v}} + [\,\mathbf{C} + \mathbf{C_c}(\alpha_n,\omega_n)]\,\dot{\mathbf{v}} \;+\; [\,\mathbf{K} + \mathbf{K_c}(\alpha_n,\omega_n)]\,\mathbf{v} \;= \mathbf{T} - \mathbf{F}(\alpha_n,\omega_n) \tag{7}$$

M and **K** are the conventional finite element mass and stiffness matrices, respectively; $\mathbf{C_c}$ and $\mathbf{K_c}$ are the time varying Coriolis and centrifugal stiffness matrices, respectively. The matrix **C** has been added to represent the internal viscous damping of the material. The vector **T** contains the unknown torques at the joints. **F** the known forces produced by the rotating frame effect.

The set of finite element equations (7) may be partitioned as follows:

$$\mathbf{M}\begin{bmatrix}\ddot{\theta}_h\\ \ddot{v}_i\\ \ddot{v}_t\end{bmatrix} + [\mathbf{C}+\mathbf{C_c}(\alpha_n,\omega_n)]\begin{bmatrix}\dot{\theta}_h\\ \dot{v}_i\\ \dot{v}_t\end{bmatrix} + [\mathbf{K}+\mathbf{K_c}(\alpha_n,\omega_n)]\begin{bmatrix}\theta_h\\ v_i\\ v_t\end{bmatrix} = \begin{bmatrix}1\\0\\0\end{bmatrix} T - \begin{bmatrix}F_h(t)\\ F_i(t)\\ F_t(t)\end{bmatrix} \tag{8}$$

where θ_h are the elastic rotations at the joints, v_t represent the elastic deflections (x,y,z) at the end-effector, and v_i are all the other internal finite element elastic degrees of freedom of the manipulator. The force vector **F** is partitioned in the same manner.

4. Inverse Dynamics

The essence of the inverse dynamics is to find the torques T at the robot joints that will cause the end of the manipulator to move along a specified nominal trajectory. The problem can be quantitatively stated as the finding of the torques T in Eq. (8) under the condition that elastic deflections at the end-effector $v_t(t)$ be zero.

Planar motions

The first and third motions are planar. In this case the best way to solve the inverse dynamics is by establishing a recursive procedure as explained in detail in reference [8]. This procedure consists in finding first the torque corresponding to the last link under the condition that the elastic displacement at the tip is zero, the next step is to compute the reactions at the hub which will be transmitted to the next link in the chain. These reactions may be obtained simply by equilibrium considerations. The procedure continues with the next link in the chain in the same manner as before with the reaction forces included. Note that this process is conceptually similar to the recursive Newton-Euler scheme for inverse dynamics of rigid robots. The method continues with the rest of the links until the torque on the first link is determined. This way of proceeding assures that the end of each link moves along the desired nominal trajectory without oscillating from it. Once the torques T have been obtained, the motions at any point of the links specified by v_i or the angles θ_h (inverse kinematics) follow from Eq (8) by a direct analysis.

Spatial Motion

In the case of three dimensional manipulators with elastic properties in all directions, there are elastic displacements that can not be controlled by the corresponding joint torque. These elastic displacements will influence the motions of subsequent links, introducing perturbations in their nominal motion. The nominal position of each link will be modified by the elastic displacement at the end of the previous link. The recursive procedure mentioned above now requires an iteration

process that will account for the displacement corrections starting with the last link. For the spatial motion at hand the manipulator does not change its configuration (except for the global rotation), and rather than using the recursive procedure, it is easier to find the solution for the three joint torques $\boldsymbol{T}$ directly from Eq. (8) under the condition that three elastic deflections at the end-effector $v_t(t)$ be zero.

The forcing terms in the right hand side of Eq. (6) depend on the velocities and acceleration profiles of the nominal motion of the link. These will have to be Fourier transformable for the problem to have a solution. Again once the torques $\boldsymbol{T}$ have been found, the motions at any point of the robot specified by v_i and the joint angles θ_h (inverse kinematics) can be readily obtained from Eq.(8) by a direct analysis. It becomes obvious at this point how the inverse dynamics and kinematics are closely coupled in the analysis of flexible robots.The torques $\boldsymbol{T}$ can be found in the frequency domain by means of an iterative numerical procedure similar to that used by Bayo et al [7-8]. In order to set up the iterative process Eq. (8) may be restated as follows:

$$\mathbf{M}\ddot{\mathbf{v}} + \mathbf{C}\dot{\mathbf{v}} + \mathbf{K}\mathbf{v} = \mathbf{l}\boldsymbol{T} - \mathbf{F} - \mathbf{C}_c(\alpha_n,\omega_n)\dot{\mathbf{v}} - \mathbf{K}_c(\alpha_n,\omega_n)\mathbf{v} \qquad (9)$$

where all the time invariant terms have been left in the L.H.S. of the equation and the time variant ones have been moved to the R.H.S. The vector $\mathbf{l}$ contain unit values for the degrees of freedom corresponding to the joint rotations and zero for the rest, as shown in Eq. (8).

The iteration process is initiated by solving Eq.(9) for the unknown torques $\boldsymbol{T}$ in the frequency domain (see [7-8] for a detailed description of this process). The first iteration is done in the absence of the last two terms involving $\mathbf{C_C}$ and $\mathbf{K_C}$ in the RHS. The first iteration will yield a displacement vector $v^1(t)$ which in turn will be used to compute $\mathbf{K_C}$ and $\mathbf{C_C}$, and the last two terms in Eq. (9). The process is then repeated with the new force vector under the constraint that $v_t(t)=0$. The iteration procedure may be stopped when the norm $\|\boldsymbol{T}_i - \boldsymbol{T}_{i-1}\|$ for the solution of two consecutive iterations, is smaller than a prescribed tolerance.

5. Simulation Analysis

Let us consider as an example a manipulator with the following characteristics:

First link: L=0.2 m, A=1.90x10^{-4} m^2, I_1=I_2= 3.5x10^{-9} m^4,
J=2.0x10^{-8} m^4, M_t=2.0 Kg, I_h=0.002 m^4

Second link: L=0.6 m, A=1.20x10^{-4} m^2, I_1=I_2= 2.2864x10^{-10} m^4,
J=4.57x10^{-10} m^4, M_t=1.0 Kg, I_h=0.0012 m^4

Third link: L=0.6 m, A=0.40x10^{-4} m^2, I_1=I_2= 8.4683x10^{-12} m^4,
J=1.69x10^{-11} m^4, M_t=0.15 Kg, I_h=0.00048 m^4

They share the following properties: E=7.11x10^{10} N/m^2, mass density = 2715 Kg/m^3, shear coefficient k=1/2 and a damping ratio of 0.002. The first frequencies of the bending modes in rd/sec of the second and third links under pinned-free conditions are: for the second link ω_1=0 (rigid body mode), ω_2=157.53, ω_3=487.55; and for the third link ω_1=0, ω_2=54.73, ω_3=181.98 and ω_4=389.93. The natural frequencies of first link are so high that it is considered as being rigid. The manipulator is modeled with 11 finite elements with a total of 67 degrees of freedom.

The first and third motions consist in straight-line tip trajectories (each one of 1 second of duration) generated according the acceleration profile shown in Fig. 5 which corresponds to a Gaussian velocity profile [12]. The second motion consists in a circular tip trajectory whose acceleration is shown in Fig. 5 also and which last 3 seconds. The solution of the inverse dynamics is not limited by the type of trajectories chosen, as long as their acceleration profiles are

Fourier transformable [9]. As shown in [7] and [12], other type of trajectories can be perfectly used. However the trajectory corresponding to a Gaussian velocity profile is selected because it diminishes the high frequency content of the input function.

The torques that need to be applied at each actuator to yield the required tip trajectory are calculated according to the procedures described above. As examples Fig. 6 shows the torque T_2 (flexible torque) for the first motion, compared to the torque needed to produce the same tip motion on an infinitely rigid link of the same mass (rigid torque). Fig. 7a and 7b show the torques T_0 and T_2 for the second motion. It is important to note that in order to track the desired trajectory the flexible torques need to be applied before the tip actually moves, as also noted in [7-8]. In addition, it may be seen also that the flexible torques have a smaller peak value, and are more spread over time than the rigid one. As a result of the inverse kinematics, Fig. 8 compares the nominal angle at joint 2 with the calculated one for the first part of the motion. These could obviously be used in a collocated feed-back control scheme.

All the calculations were performed using a SUN 160 workstation. The total time required for the computation of these torques for all the three motions was approximately 20 seconds. The computational burden is mostly due to the solution of the complex sets of equations and the use of the fast Fourier transform. The computed torques produce the desired tip trajectory without overshoot or residual oscillations. A forward dynamic analysis and graphics simulation are performed yielding the results shown in Fig.9 and 10. It may be observed how both links bend along their motion. However, their ends follow the specified nominal path. Finally Fig. 12 illustrates the motion of the end-effector when the rigid torque at joint 0, corresponding to the second motion, is input to the system. Although the rigid torque is smooth the tip still vibrates, and this points out the fact that smooth trajectories or torques are not enough to eliminate residual vibrations.

6. Conclusions and Acknowledgement

A procedure has been presented for the inverse dynamics and kinematics of a three degree of freedom spatial manipulator. The proposed algorithm calculates the torques required to move the end effector through a specified trajectory while avoiding tip oscillations. The tip trajectory acceleration profile should be Fourier transformable. The technique is demonstrated through simulation yielding very good results. The algorithm converges very rapidly in all the cases considered.

The use of the fast Fourier transform, solution of complex equations and the necessity to iterate to obtain the required solution preclude this method from being used in real time control. However, it can still be used in open-loop control and other close-loop control strategies. Currently, under investigation are time domain algorithms to be implemented in multi-processors computer architectures which will substantially reduce the computational time.

The authors would like to acknowledge the support of this work by NATO, grant number 0877-87, and by the National Science Foundation, grant number 8421415, through the Center for Robotics Systems in Microelectronics.

References

1. R. H. Cannon and E. Schmitz, "Initial Experiments on End-Point Control of a Flexible One-Link Robot," *Int. J. Robotics Res.*, Vol. 3, No. 3, pp. 62-75 (1984).

2. Y. Sakawa, F. Matsuno, and S. Fukushima, " Modeling and Feedback Control of a Flexible Arm," *J. Robotic Syst.*, Vol. 2, No. 4. pp. 453-472 (1985).

3. F. Harashima, T. Ueshiba ,"Adaptative Control of Flexible Arm Using the End-Point Position Sensing". Japan-USA Symposium on Flexible Automation. Osaka, Japan. Vol. 1, 225-229 (1986).

4. P. Kotnik, S. Yurkovik and Ü. Özgüner, "Acceleration Feedback Control for a Flexible Robot Arm," *J. Robotic Syst.*, Vol. 5, No. 3, pp. 181-196 (1988).

5. D.Wang and M. Vidyasagar, "Control of a Flexible Beam for Optimum Step Response," *Proceedings of the IEEE International Conference on Robotics and Automation*, Vol. 3, pp. 1567-1572 (1987).

6. E. Bayo, "A Finite-Element Approach to Control the End-Point Motion of a Single-Link Flexible Robot," *J. Robotic Syst.*, Vol. 4, No. 1, pp. 63-75 (1987).

7. E. Bayo, R. Movaghar and M. Medus, "Inverse Dynamics of a Single-Link Flexible Robot. Analytical and Experimental Results". *Int. J. of Robotics and Automation.* Vol. 3, No. 3, pp.150-157, (1988).

8. E. Bayo, M. Serna, P. Papadopoulos, J. Stubbe "Inverse Dynamics and Kinematics of Multi-Link Elastic Robots. An Iterative Frequency Domain Approach" Report # UCSB-ME-87-7 Mechanical Engineering Department, University of California Santa Barbara, Dec 1987. To appear in the *International Journal of Robotics Research.*

9. Moulin H. and Bayo E. "On the Accuracy of End-Point Trajectory Tracking for Flexible Arms by Non-Causal Inverse Dynamic Solutions," Report # UCSB-ME-88-9 Mechanical Engineering Department, University of California Santa-Barbara, Nov 1988.

10. A. De Luca and B. Siciliano, "Joint-Based Control of a Nonlinear Model of a Flexible Arm," Proc. American Control Conference. Atlanta. (July 1988).

11. K. J. Bathe, *Finite Elements Procedures in Engineering Analysis*, Prenctice-Hall, Englewood Cliffs, NJ, 1982.

12. Bayo, E. and Paden, B. "On Trajectory Generation of Flexible Robots". *Journal of Robotic Systems*. Vol. 4 No. 2, pp. 239-245. Spring 1987.

figures

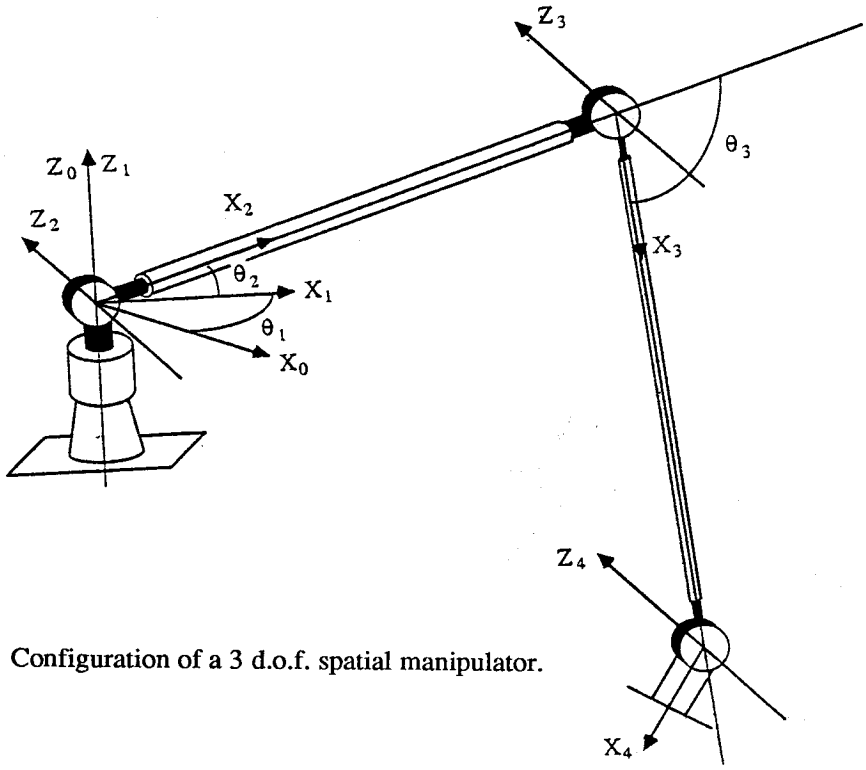

1. Configuration of a 3 d.o.f. spatial manipulator.

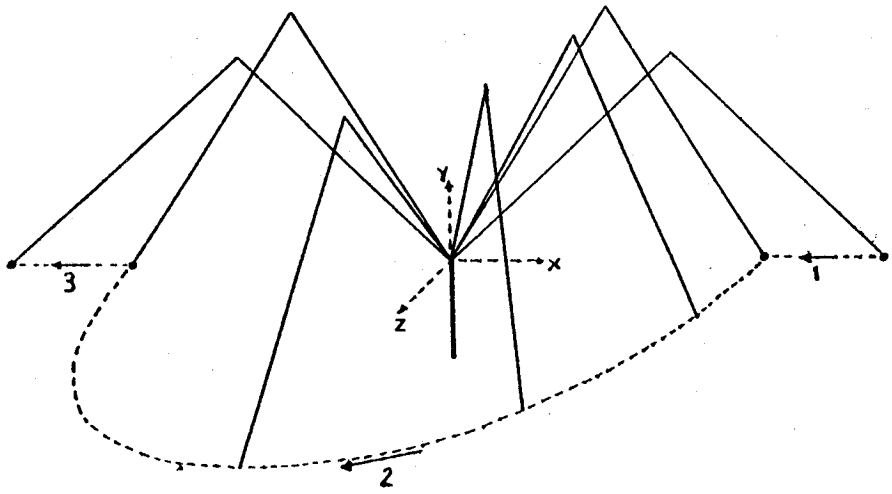

2. The three parts of the motion.

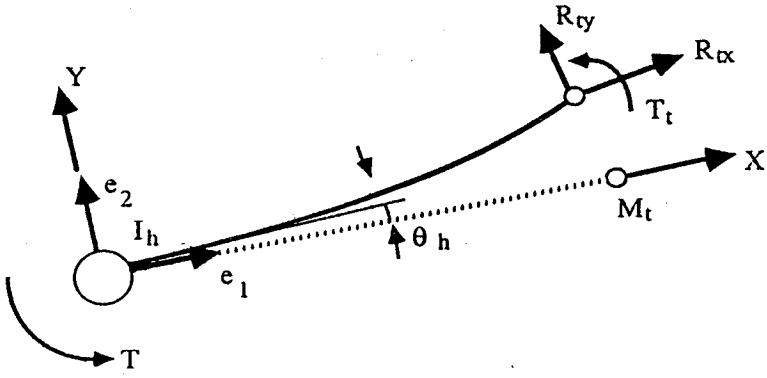

3. Deformation of a link in planar motion.

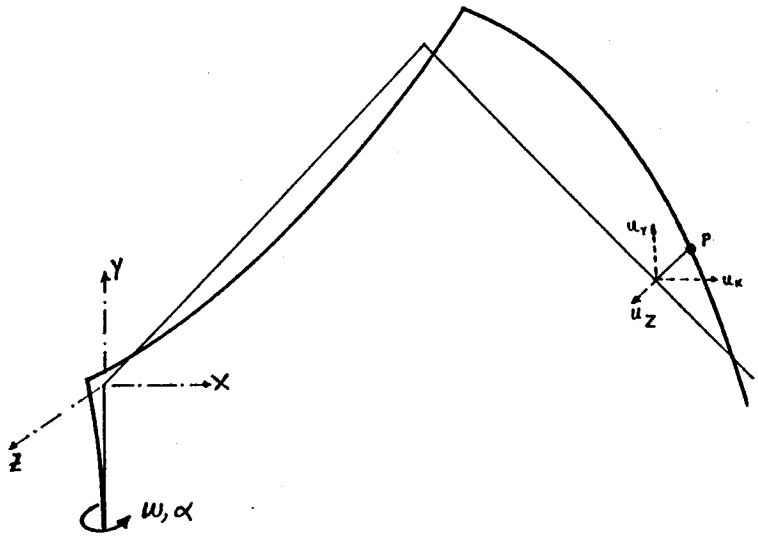

4. Deformation of the robot in the spatial motion.

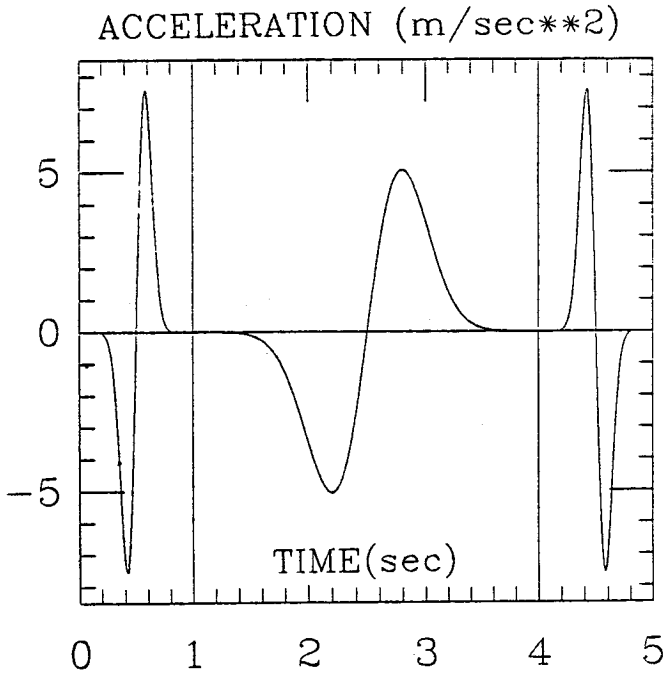

5. Acceleration profiles for the three motions.

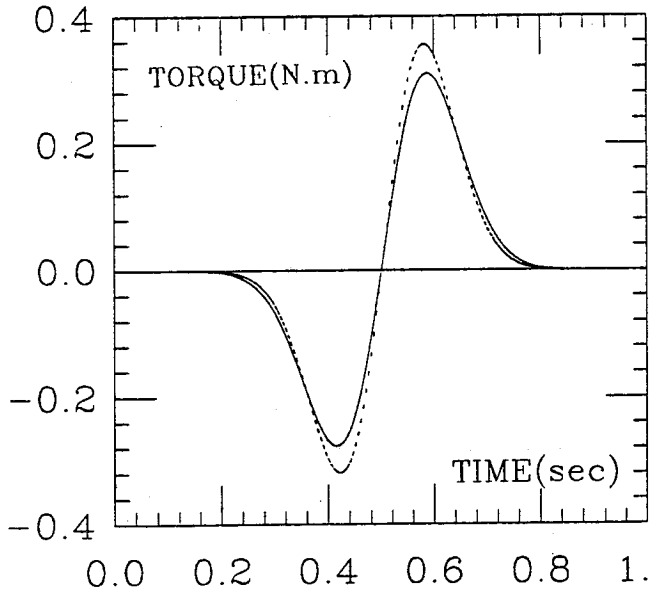

6. Joint 2. First part of the motion.
Rigid torque (dotted) vs. flexible torque (solid).

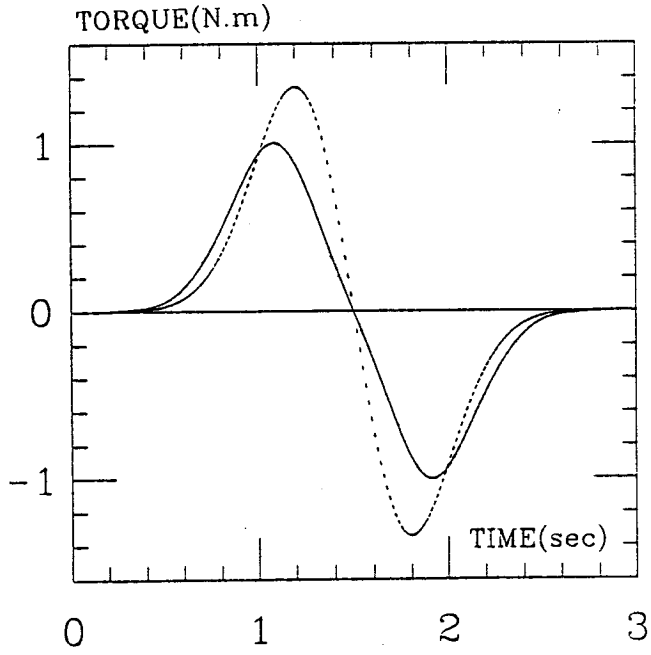

7a Joint 0. Second part of the motion.
Rigid torque (dotted) vs. flexible torque (solid).

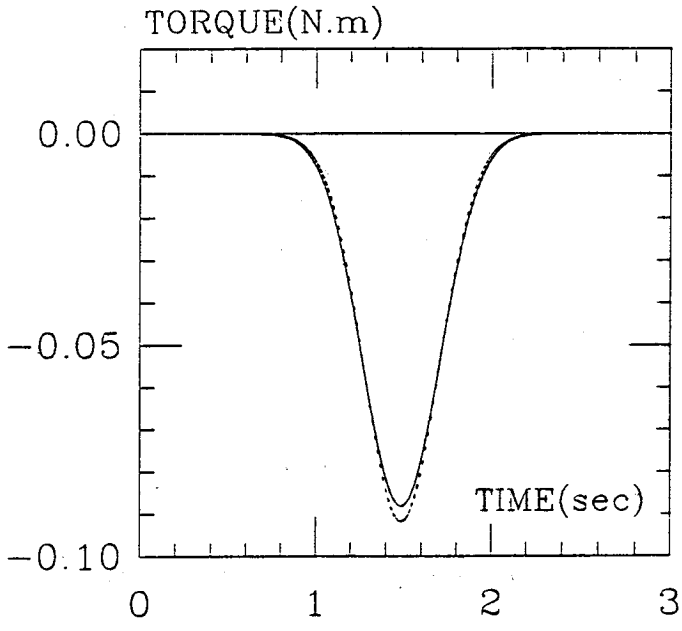

7b Joint 2. Second part of the motion.
Rigid torque (dotted) vs. flexible torque (solid).

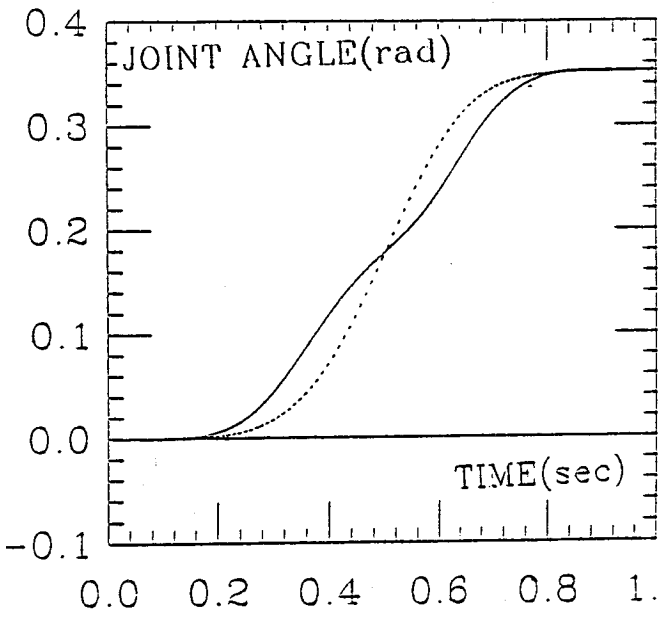

8 Joint 2. First part of the motion.
Nominal (dotted) vs. calculated (solid) joint angles.

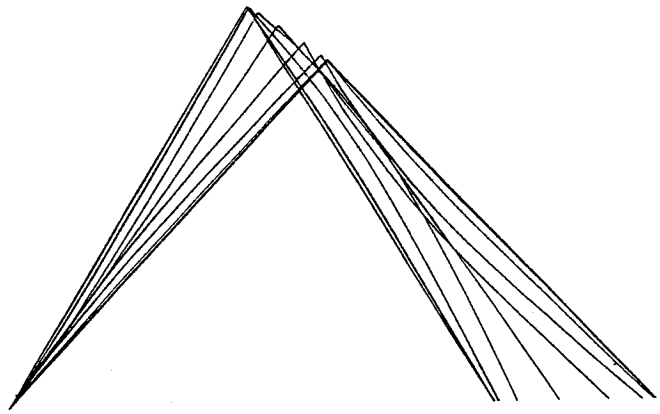

9. Simulation of the first part of the motion.

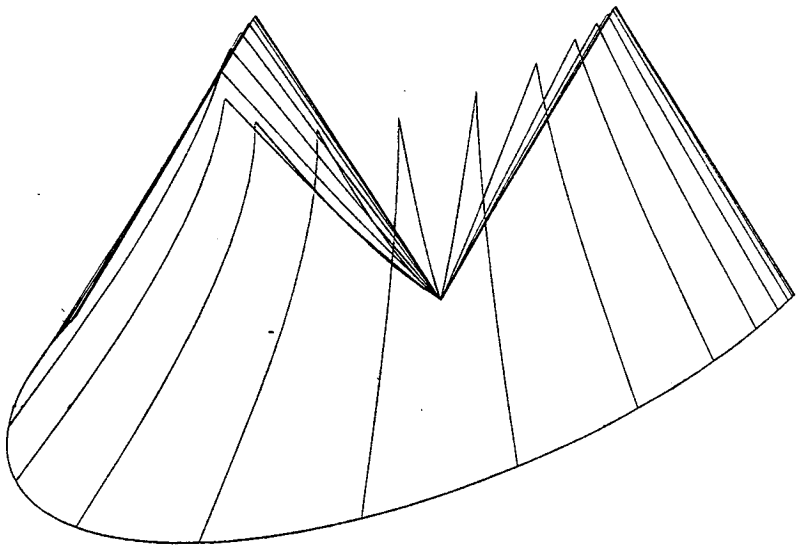

10. Simulation of the second part of the motion.

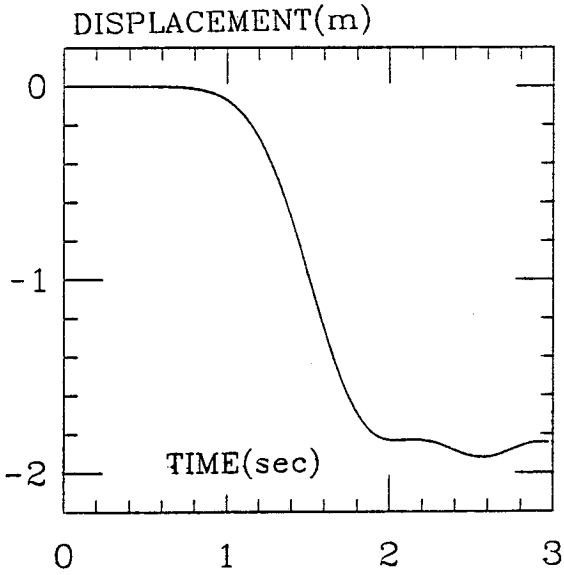

11. Vibration at the end-effector when using the rigid torque. Second part of the motion.